

Application of laser assisted technologies for fabrication of functionally graded coatings and objects for the International Thermonuclear Experimental Reactor components

I. Yadroitsev, Ph. Bertrand, B. Laget, I. Smurov *

Ecole Nationale d'Ingénieurs de Saint-Etienne (ENISE), DIPI Laboratory, 58 rue Jean Parot, 42023 Saint-Etienne cedex 2, France

Abstract

The technology of selective laser melting (SLM) was applied for manufacturing of net shaped 3D objects from different powders Inco 904L, Ni625, Cu/Sn, W. Performance and limitations of SLM technology for fabrication of elements of cooling systems in International Thermonuclear Experimental Reactor (ITER) installations were analysed. The developed technology was applied for fabrication of the inner surface of divertor thimbles. Two-component objects (stainless steel/Cu) were fabricated in a two-step manufacturing cycle. Direct laser manufacturing (DLM) with coaxial powder injection was applied for fabrication of thick functionally graded coatings and 3D objects from metallic powder. One of the advantages of DLM is the possibility to build functionally graded coatings and 3D objects in a one-step manufacturing cycle by using a 2-channel powder feeder. Several models with different types of material gradients (smooth, sharp, periodic) and multi-layered structures were manufactured from stainless steel, Stellite, Cu and W alloys.

© 2007 Elsevier B.V. All rights reserved.

PACS: 42.62.-b; 64.70.Dv; 28.52.-s

1. Introduction

Consolidation of powder by local laser heating/melting is becoming a promising manufacturing technique because of easy control over both powder deposition/transport and laser radiation. The current activities in laser assisted direct manufacturing are mostly centered around the two recent developments, namely, (a) selective laser melting for manufacturing parts with complex three-dimensional

(3D) shape and (b) synthesis of functionally graded materials (FGM) by injection of powder blends with variable composition coaxially with the laser beam. Selective laser sintering/melting (SLS/SLM) technology makes it possible to create fully functional parts directly from metals without using any intermediate binders or any additional processing steps after the laser sintering operation. The laser assisted technology of free-form manufacturing of FGM objects represents one of the most promising directions to solve challenging industrial problems. This approach promises to extend dramatically the freedom of design and manufacturing allowing, for example, to create an object with desired shape, internal structure

* Corresponding author. Tel.: +33 4 7791 0161; fax: +33 4 7774 3497.

E-mail address: smurov@enise.fr (I. Smurov).

and engineered composition including appropriate protective coating in a single fabrication step [1,2].

2. Selective laser melting

2.1. Experimental set-up

SLS/SLM machine consists of a table to which two containers are attached. The bottom of each container is a piston. Initially, one of the containers (left) is filled with a powder and the other (right) is empty with the piston at the level of the table. The process is started with a thin powder layer deposition in the right container. First, the left piston is increased and the right piston is decreased by the layer thickness. Then, a roller scrapes powder from left to right. The deposited layer is then scanned with the laser beam, which causes local heating and consolidation of powder. The cycle of powder deposition/laser scanning is repeated many times resulting in a solid 3D part immersing into loose powder [3]. The essential operations are deposition of a thin powder layer and laser beam scanning over its surface. Powder binding mechanisms, such as melting and solid-state or liquid-phase sintering, strongly depend on the laser induced heating and applied powder [4–6].

Experiments were carried out on PHENIX-100 machine: 50 W fiber laser, powder is spread by a roller over the surface of a build cylinder with 100 mm diameter. Different commercial powder were used: Inox 904L, Ni625, Cu/Sn, W.

2.2. Results and discussion

The SLM technology was applied for fabrication of several model objects that can be used in cooling systems of ITER. The ‘models’ have a particular geometry: (a) thin walls (to intensify heat exchange) and (b) internal cooling channels.

An example of a thin-walled model is presented in Fig. 1 the box of $20 \times 20 \times 5$ mm with inner compartment walls of the minimal possible thickness ($140 \mu\text{m}$ in the present case). Long term stability of SLM process was controlled by fabrication of large-size thin-walled objects during 36 h.

Two different models with internal cooling channels are presented in Fig. 2. The average bulk porosity is about 1%.

Another example corresponds to ITER problematic where He will be used as a coolant. The goal is to augment the heat transfer coefficient in finger-shaped divertor elements. The inner surface of a thimble should have a particular geometry. The results of fabrication of a model with similar geometry are presented in Fig. 3. Note that a single step manufacturing method was applied.

Combination of steel–Cu elements in the cooling systems is a conventional approach. To demonstrate the potential of SLM technology to fabricate an object from stainless steel with internal cooling channels from Cu, two-component objects (stainless steel/Cu) were fabricated in a two-step manufacturing cycle with PHENIX-100 machine (Fig. 4).

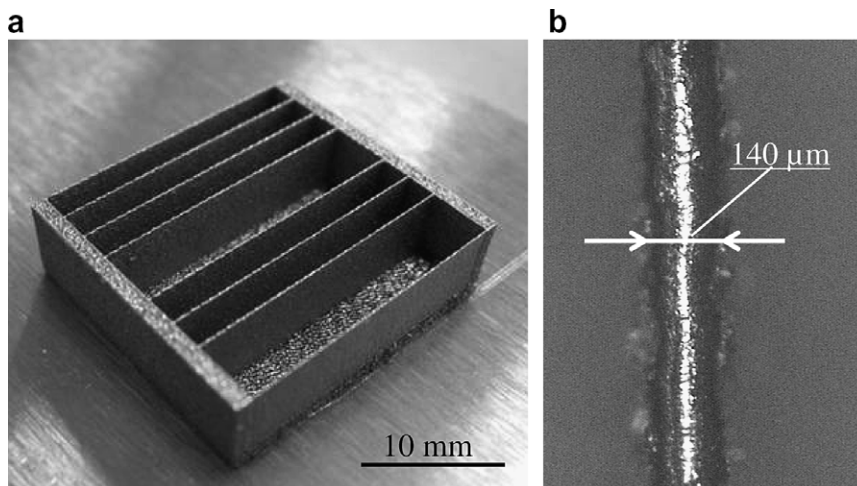


Fig. 1. Thin-walled model fabricated by SLM technology from INOX 904L powder: (a) general view; (b) top view of the thin wall.

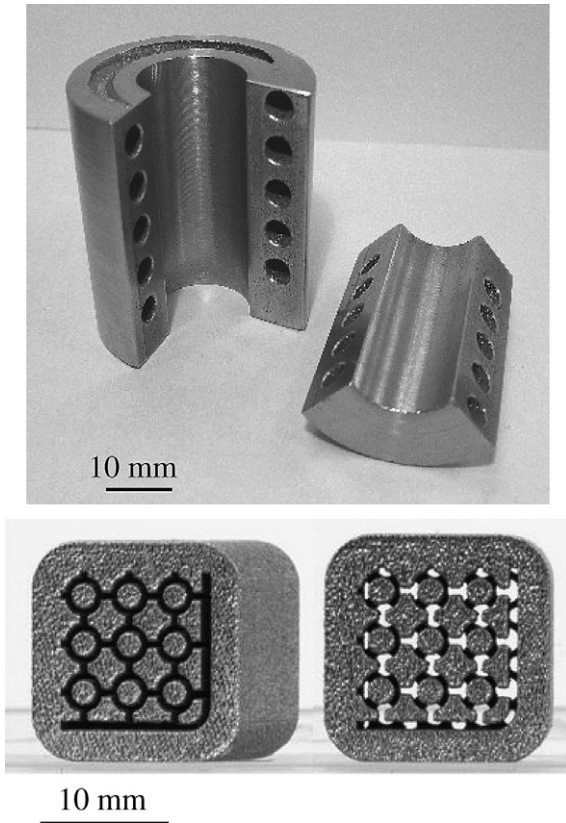


Fig. 2. Two different models with internal cooling channels fabricated by SLM technology.

3. Direct laser manufacturing

3.1. Experimental set-up

Experimental set-up consist of laser source, laser beam delivery system, powder feeding system, coaxial nozzle, and numerically controlled 5-axes table.

- Laser sources: CW Nd:YAG HAAS 2006D, output power up to 2 kW; pulsed-periodic Nd:YAG HAAS HL62P (average power is 60 W). The radiation is delivered to the working zone by optical fiber.
- Powder feeder: 2-channel MEDICOAT, powder feed rate can be adjusted separately for each channel. Argon is used as the carrying gas.
- Coaxial nozzle: the advantage of the coaxial injection is a small heat affected zone (HAZ) and the possibility of multidirectional cladding due to radial symmetry between the laser beam and the powder flux. The shielding gas (Ar) sur-

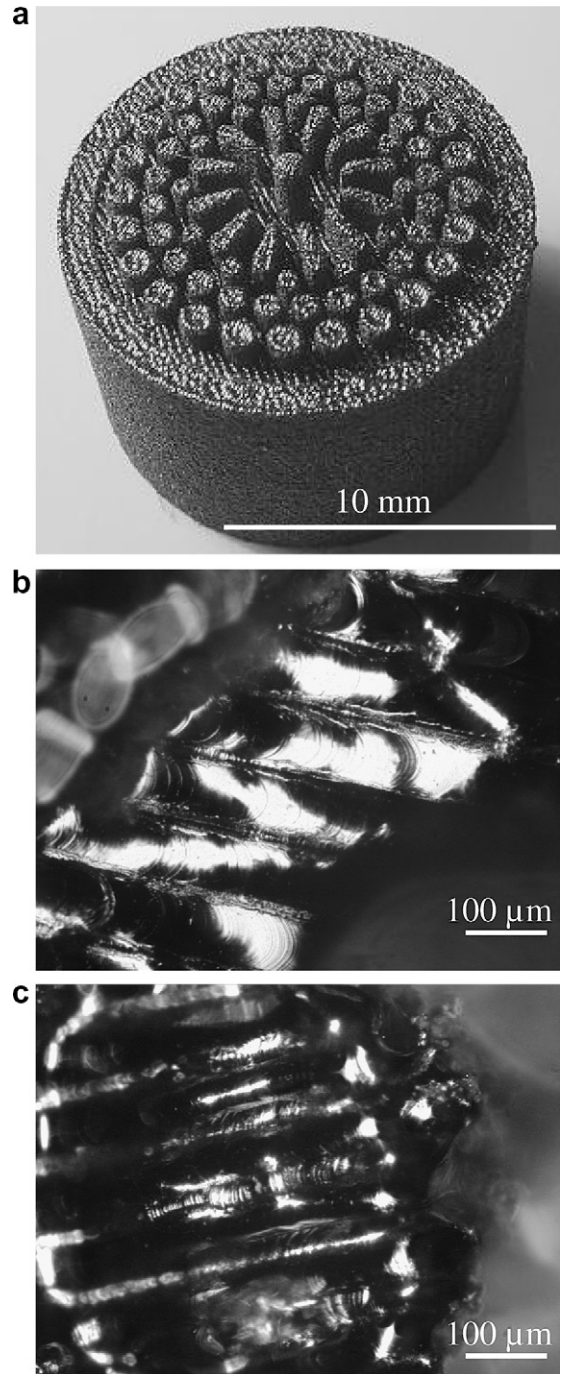


Fig. 3. Prototype of the cooling cell fabricated by SLM technology: (a) general view; (b) surface of the cooling cell in between the pins; (c) surface of one of the pins.

rounds, focuses and protects the powder flow and the melting pool from oxidation [7–9,13].

- CNC center LASMA 1054 is used to move the sample and the nozzle with positioning accuracy up to 1 μ m.

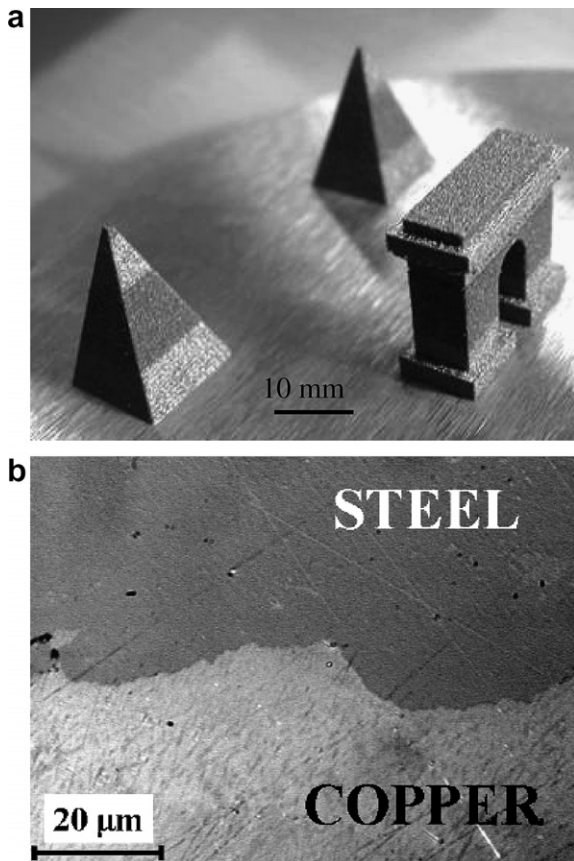


Fig. 4. Bi-material models (stainless steel/Cu) fabricated in a two-step SLM manufacturing cycle: (a) general view, (b) cross-section of the sample.

Composition gradient is achieved by changing the powder flow content during the deposition process, while keeping the total powder volumetric flow and FGM growing rate constant. The performance of the twin powder feeder allows mixing two different types of powder, thus creating binary compound functionally graded structures.

3.2. Applied materials

The following powders were tested for producing 3D objects with/without material gradient: Fe–Cu (60/40 wt%) nanocomposite powder, $-47 + 12 \mu\text{m}$; (fabricated by MBN), WC/Co (70/30 wt%) nanostructured powder, $-75 + 38 \mu\text{m}$ (fabricated by MBN), 430L stainless steel powder, $-75 + 22 \mu\text{m}$; (Osprey Metals), Bronze (10Al 1Fe) Spheroidal, Gas Atomized $-45 + 10 \mu\text{m}$; (Osprey Metals), Stellite Grade 12 powder, $-150 + 53 \mu\text{m}$; (Hoganas),

WC/Co (12 wt%) composite powder $-53 + 11 \mu\text{m}$; (Sulzer Metco).

3.3. Applied optical diagnostics

To produce 3D FGM object, materials with different thermo-physical properties are applied. For this reason, they interact with the laser beam in different ways thus leading to changes in temperature, dimensions of the melting pool and finally, to distortion of the part's geometry. Thus, the appropriate diagnostic equipment should be applied to control temperature and geometrical dimensions of the workpiece. A set of diagnostic equipment including 2D monochromatic and single spot multi-colour pyrometers and a CCD-camera based diagnostic tool for measurement of the particles size and velocity was used in process optimisation and control [12].

3.4. Elaboration of 3D samples with functionally graded material distribution

To determine the optimum parameters of the DLM process, a great number of single-material samples was fabricated. Typical geometry corresponds to cylinders and walls. Analysis of the samples made of stainless steel 316L showed that the layers have a fine grain structure with no cracks or other defects. The structure was typical for primary austenite solidification in austenitic stainless steel.

3.5. Bi-material compositions

A number of samples (with 'wall' shape) was produced with smooth or sharp variations in material content. The minimal size of transition zone between two different materials is considered as the gradient spatial resolution.

The following types of graded materials were realized using binary compound (stainless steel and Stellite): smooth gradients (Fig. 5), sharp multi-layered gradients (Fig. 6), smooth multilayered gradients.

The achieved sample wall thickness is in the range of 200–300 μm . It is approximately 1.5 times larger than the laser spot diameter. The wall height is up to 12 mm and the length is up to 45 mm.

Fig. 5 represents smooth gradient from stainless steel to Stellite. Stellite has a dendritic microstructure that consists of Co–Cr–W solid solution, the interdendritic region corresponds to carbides

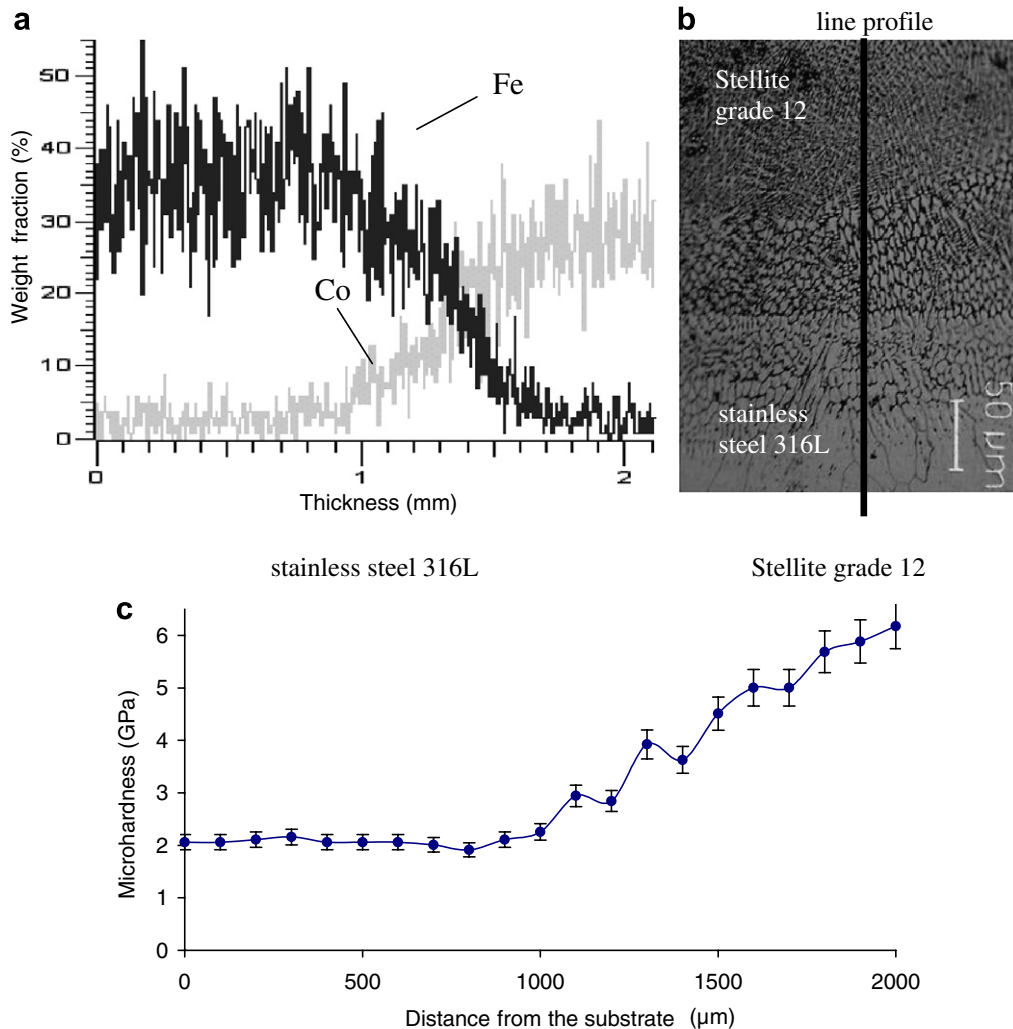


Fig. 5. Sample with smooth gradient transition stainless steel–Stellite: (a) distribution of the components in the longitudinal direction: black curve represents concentration of Fe (from steel), gray curve represents Co (from Stellite); (b) cross-section, polished, etched; (c) microhardness.

($M_{23}C_6$, M_7C_3). The grain size is about 1–3 μm. Note that thickness of the layer deposited by one passage of the laser beam is about 50 μm. The laser power density was gradually changed to obtain uniform layer thickness during the fabrication process. It is known [10] that Stellite is a two-phase material with a relatively soft matrix and a reinforcement phase consisting of carbides, intermetallic compounds, e.g. Co_3W with dislocation–dislocation interactions which greatly determine mechanical properties. The increase of the stainless steel concentration diminishes the contribution of the above-mentioned factors and leads to a gradual change of mechanical properties. The microhardness profile

along a graded wall is shown in Fig. 5(c). One may note that microhardness increases continuously with Stellite concentration. It is in a good agreement with SEM analysis. In this case the transition zone is wide and it is of the same order as the sample size.

Metallographic observation of the cross-section shows dendrites that sometimes penetrate through two or three deposited layers. Along with this the last layer always represents a finer grain structure with cell dimensions not more than 1.2–1.5 μm. It is due to the fact that the heat affected zone (150 μm) is greater than the layer thickness (50 μm) and previously deposited layers are heated and cooled several times with gradual decrease in

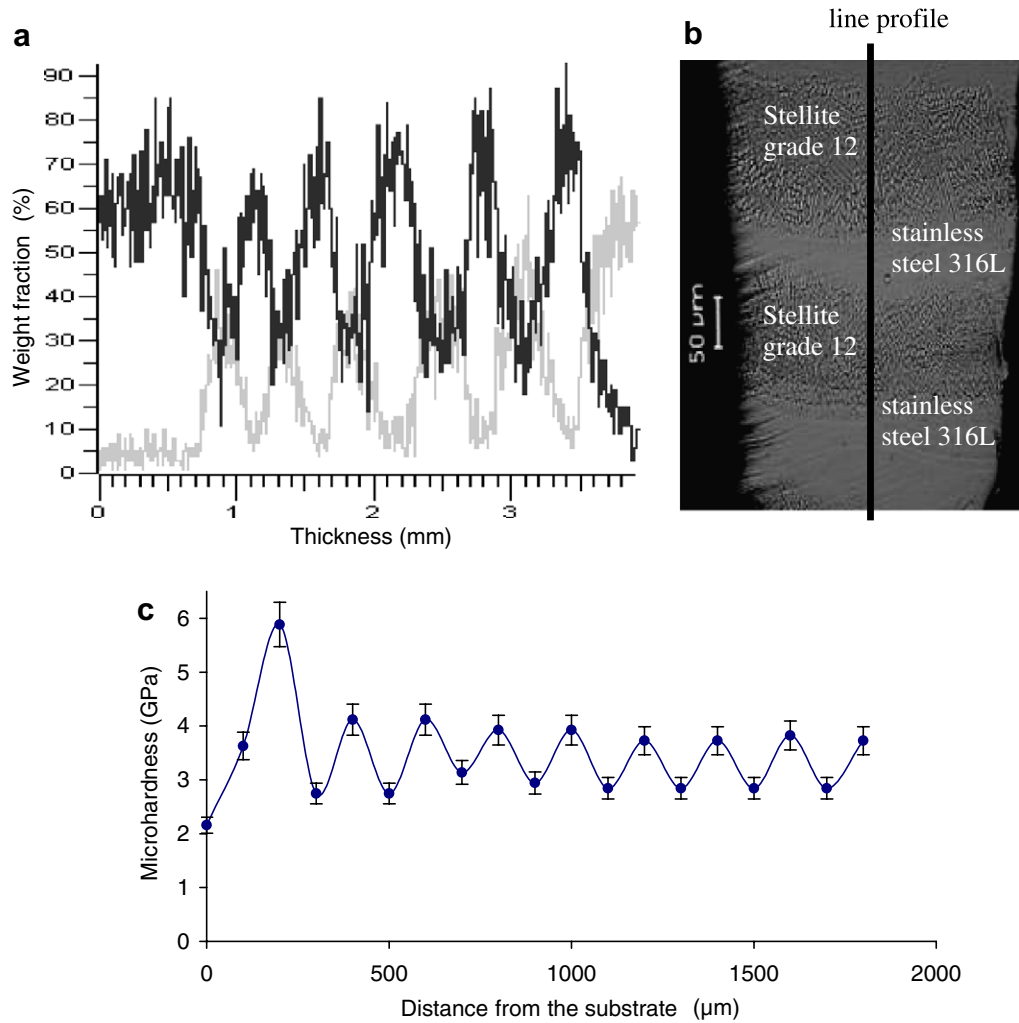


Fig. 6. Sample with sharp gradient multilayered structure stainless steel–Stellite: (a) distribution of the components in the longitudinal direction: black curve represents concentration of Fe (from stainless steel), gray curve represents Co (from Stellite); (b) cross-section, polished, etched; (c) variation of microhardness.

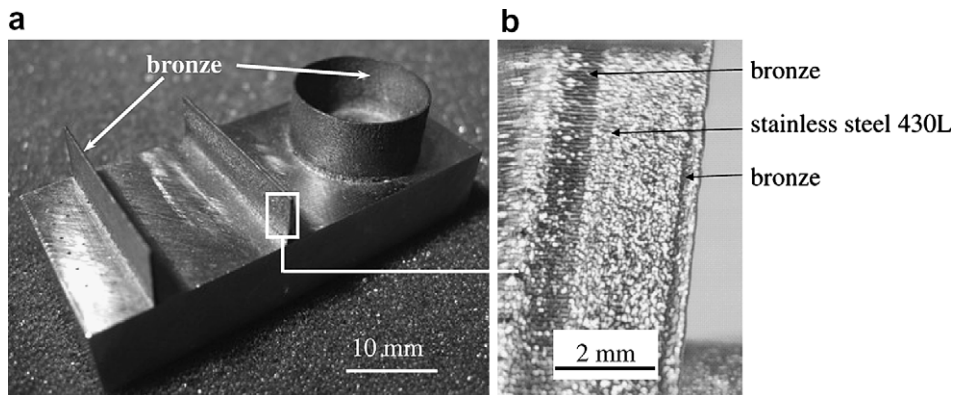


Fig. 7. Samples fabricated by the pulsed-periodic HL62P laser from stainless steel and bronze powder: (a) general view of the thin-walled models (wall thickness is 400 μm), (b) graded wall (transition between bronze and stainless steel).

the cooling rate. The upper layer consists of particles melted and solidified only once thus creating a fine microstructure.

Possible variation of gradient resolution was studied on the sharp gradient multilayered structure shown in Fig. 6. It is built up by repeating a sequence of layers {stainless steel–Stellite}. The gradient resolution revealed by SEM analysis is about 30 μm .

The next structure is built up by repeating a sequence of three different layers {stainless steel–Stellite/stainless steel mixture (50/50 vol.%)–Stellite layers}. This combination of layers allows production of multilayered structures with rapid transition between different materials. Such type of FGM could be useful for improvement of mechanical properties, e.g. shock strength [11].

It is possible to conclude that by variation of coaxially injected powder composition the following typical gradient structures were obtained:

- Smooth transition from one pure alloy, say A, to another one, say B, on a characteristic length of several millimeters (characteristic size of the fabricated object).
- Multi-layered structures with periodic variation of alloys A and B, characteristic length of composition variation is up to a single layer thickness, i.e. about 30 μm .
- Three consecutive repetitive layers (A/50%A + 50%B/B) with a period about 150 μm .

The pulsed-periodic laser HL62P was used to fabricate samples from bronze and stainless steel 430L with the wall thickness of 400 μm (Fig. 7). The first wall is made from pure bronze, another wall is made with a gradient between bronze and stainless steel, the cylinder is made from bronze.

3.6. Multi-material compositions

The fabricated FGM sample, Fig. 8, consists of four different zones having the following composition: zone I – Stellite 12 plus FeCu plus WC/Co, zone II – Stellite 12 plus FeCu, zone III – stainless steel 430L, zone IV – Stellite 12.

This sequence of four different zones represents one of the typical conception of the FGM object: (a) internal areas are fabricated from commonly applied structural materials, as for example stainless steel and Stellite, (b) smooth gradient zone with addition of ductile FeCu and finally, (c) fabrication of the protective coating, in the present case by

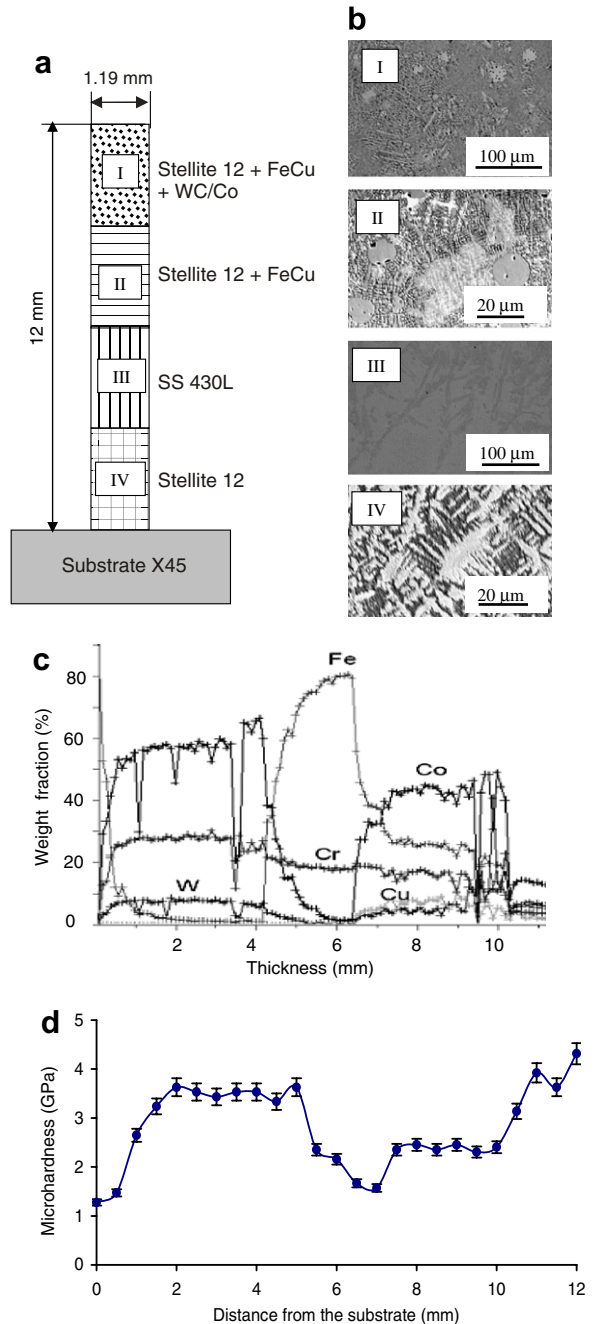


Fig. 8. Multi-component wall: (a) general scheme of the graded wall (cross section); (b) SEM (secondary electrons) images of the four different zones; (c) distribution of the elements by SEM analysis; (d) microhardness distribution along the graded wall (bottom–up).

addition of the wear-resistant WC/Co reinforcement phase. The function of nanostructured FeCu powder is to stop crack propagation and to increase allowable shock load due to its ductility.

The longitudinal distribution of characteristic elements is derived from SEM analysis and corresponds to the composition of initial powder blends.

The dependence of microhardness vs. distance from the substrate shows plain growth of hardness from the substrate 1.28 GPa through the heat affected zone and the intermediate zone to 3.43–3.83 GPa corresponding to the Stellite zone. Then the value of microhardness drops to approximately 1.47–1.96 GPa (the stainless steel zone) and after that keeps stable within 2.26–2.65 GPa, which corresponds to the Stellite–Fe/Cu zone. Saw-tooth growth of microhardness in the last zone is a result of inhomogeneity of composition in the Stellite–Fe/Cu–WC/Co zone. In this case, two different powder mixtures – Stellite 12 (50 vol.%) + Fe/Cu (50 vol.%) and WC/Co/Cr – were supplied through two different channels of the powder feeder and mixed in the nozzle before injection. In general, addition of WC-based composite powder results in significant increase in hardness.

Microstructure of the fabricated layers is the following: dendritic in the case of Stellite (IV), coarse-grained (ferrite structure) in the case of chromium stainless steel and mainly columnar in the case of Stellite–Fe/Cu mixture (II). In the layer (I), areas of different microstructure can be observed (areas with fine-grained structure, areas with the structure similar to the one in the layer II and small spherical inclusions of Cu), which predetermines the saw-tooth change of microhardness within the layer.

4. Conclusions

SLM technology shows considerable progress to meet the challenge for fabrication of complex shape functional models from commercial metallic powders. One of the principle criteria is the accuracy of fabrication with respect to the desired dimensions of the final product. SLM is the promising method for fabrication of elements of cooling systems for ITER.

A number of FGM samples is produced by coaxial powder injection. Materials are engineered by appropriate change of the powder composition during DLM process. The different types of gradients:

sharp, smooth and multilayered were realized from the following materials and their blends: stainless steel 316L, Stellite grade 12, nanostructured FeCu, nanostructured WC/Co, CuSn, bronze. The originality of the applied method of manufacturing is that in general all types of gradients could be realized within the same sample and in a single-step process.

The pulsed-periodic radiation is shown to be preferable to the continuous one due to smaller HAZ, higher cooling rates and possibility to precisely control the process by appropriate change of pulse parameters.

The transition zone between different compositions depends on the process parameters and can be varied in a wide range starting from 10 μm . The minimal FGM wall thickness obtained in this study is 200 μm .

DLM technology extends dramatically the freedom of design and manufacturing of various elements for ITER components.

References

- [1] Terry Wohlers et al., Wohlers Report 2005, Rapid Prototyping, Tooling and Manufacturing State of the Industry, Annual Worldwide Progress Report.
- [2] W. Lengauer, K. Dreyer, *J. Alloy. Compd.* 338 (2002) 194.
- [3] D.L. Bourell, H.L. Marcus, J.W. Barlow, J.J. Beaman, *Int. J. Powder Metall.* 28 (1992) 369.
- [4] A. Simchi, F. Petzoldt, H. Pohl, *Int. J. Powder Metall.* 37 (2001) 49.
- [5] J.-P. Kruth, P. Mercelis, J. Van Vaerenbergh, L. Froyen, M. Rombouts, *Rapid Prototyping J.* 11 (2005) 26.
- [6] Y.P. Kathuria, *Surf. Coat. Technol.* 116–119 (1999) 643.
- [7] Xiaolei Wu, *Surf. Coat. Technol.* 115 (1999) 111.
- [8] J. Lin, *Opt. Laser Technol.* 31 (1999) 233.
- [9] J. Lin, *Opt. Laser Technol.* 31 (1999) 251.
- [10] J.L.M. Otterloo, J.T.M. de Hosson, *Scripta Mater.* 36 (1997) 239.
- [11] I.-W. Chen, E.J. Winn, M. Menon, *Mater. Sci. Eng. A317* (2001) 226.
- [12] M. Doubenskaya, Ph. Bertrand, I. Smurov, *Thin Solid Films.* 453&454C (2003) 477.
- [13] A. Yakovlev, Ph. Bertrand, I. Smurov, Development of 3D functionally graded models by laser-assisted coaxial powder injection, laser-assisted micro- and nano-technologies 2003, in: V.P. Veiko (Ed.), *Proceedings of SPIE*, Bellingham, WA, 2004, p. 220.